DESIGN AND EXPERIMENTAL RESEARCH ON THE END EFFECTOR OF FRUIT ORCHARD COMB-TYPE FLOWER THINNING

/

果园梳齿式疏花末端执行器设计与试验研究

Caiqi HU*[1,2], Yechao HAN[1,2], Yichen LI[1,2], Junhao LI[1,2], Pengyu LIU[1,2], Siyuan ZHENG[1,2]
[1)] College of Mechanical and Electrical Engineering, Qingdao Agricultural University, Shandong / China
[2)] Shandong Provincial Key Laboratory of Smart Agricultural Equipment for Protected Horticulture
Tel: 8613616397874; E-mail : hucaiqi@163.com
Corresponding author: Caiqi HU
DOI: https://doi.org/10.35633/inmateh-76-87

Keywords: *mechanical flower thinning; simulation analysis; orchard test; smart horticulture*

ABSTRACT

Flower thinning is an important agricultural process in orchards. To address issues such as insufficient thinning accuracy and the need for secondary operations in traditional orchard thinning mechanisms, and to meet the agricultural demands for precise flower thinning, this study designs a comb-type flower thinning end effector based on the physical characteristics of the flowers and the agronomic requirements for thinning. This study adopts a flower thinning method combining thinning leaf spring piece and comb teeth. By optimizing the design of the spring piece dimensions, the study first systematically analyzes the force characteristics of the spring piece during the working process, as well as the force conditions of the flowers under different operating conditions, to identify the key factors affecting flower abscission. Next, ADAMS software is used for rigid-flexible coupling dynamic simulation analysis to determine the optimal working speed of the key flower thinning device as 230–250 r/min. Finally, field tests were conducted to verify the working reliability of the flower thinning machine. The test results show that the machine meets the expected design goals, providing technical support for efficient and precise flower thinning operations in orchards.

摘要

疏花是果园工作中重要的农艺过程，为解决传统果园疏花机构存在的疏花精度不足、需二次作业等问题，满足果园精确疏花的农艺需求，本研究基于花朵物理特性与疏花农艺要求，设计了梳齿式疏花末端执行机构。本研究采用疏花弹片与梳齿相结合的疏花形式，通过对弹片尺寸进行优化设计，首先系统分析弹片在工作过程中的受力特性，以及花朵在不同作业工况下的受力情况，明确影响花朵脱落的关键影响因素。其次，运用 ADAMS 软件进行刚柔耦合动力学仿真分析，确定疏花关键装置的最佳工作转速为 230~250r/min。最终通过田间试验对疏花机的工作可靠性进行验证，试验结果表明该疏花机达到预期设计目标，为果园高效精准疏花作业提供了技术支撑。

INTRODUCTION

Flower thinning is an important step in the growth process of apple trees; it can not only improve fruit quality *(Dennis et al., 2011)* but also effectively prevent the problem of yield reduction caused by excessive fruit load that burdens the tree *(Liu et al.,2018)*. Currently, traditional manual flower thinning methods mainly rely on manual operations, including pinching and flower sequence rubbing methods *(Cheng et al., 2018; Wang and Liu, 2020; Cheng et al., 2020)*. Manual flower thinning has high labor intensity and low efficiency *(Pan et al., 2021)*. Chemical flower thinning has issues with pesticide residues and is easily influenced by environmental factors, fruit varieties, and other variables *(Robinson and Lakso, 2011; Cheryl and Karen, 2011)*. Manual flower thinning still plays an important role in modern orchard management, but it can no longer meet the demands of modern agriculture for fruit quality and production efficiency *(Sui et al., 2024)*. To address this issue, mechanized flower and fruit management has become one of the urgent problems that farmers need to solve. Among them, the development and application of flower thinning machines has become a hot topic in modern orchard management *(Lan et al., 2020; Chen et al., 2018; Kang et al., 2019)*.

Currently, flower thinning devices are mainly classified into three types: manual, semi-automatic, and intelligent *(Lei et al., 2023)*. The development of orchard flower thinning machinery in China is still immature, and existing research has mainly focused on the development of airborne flower thinning mechanisms.

Li Jun et al. from South China Agricultural University *(Li et al., 2016)* designed a suspended electric flexible flower thinning machine. Wang Qiang et al. from Hebei Agricultural University *(Wang et al., 2018)* developed a mechanical flower thinning device for northern dwarf rootstock high-density orchards. Liu Huanwei et al. from Qingdao Agricultural University *(Liu et al., 2025)* developed a crawler-type double-arm apple flower thinning machine based on profile theory. Research on flower thinning machinery started earlier abroad. Recently, *Alberto et al., (2018),* developed a large flower thinning machine. Lyons et al., *(2015),* designed a selective automatic flower thinning device and a novel AI controller for a mechanical flower thinning device has been proposed *(Matache et al., 2024),* which integrates the ZED 3D camera and a custom-trained YOLO9 algorithm. It can detect and count flowers in real-time and automatically adjust the thinning rotor speed based on density to achieve the desired thinning ratio.

Currently, mainstream flower thinning equipment faces prominent issues such as poor selectivity, large body size, and high mechanical damage rates. To improve the accuracy of mechanical flower thinning, this study designed a comb-tooth type flower thinning end effector. Through research and analysis of the mechanical characteristics of flowers in the field, a flower thinning structure combining a spring piece and comb teeth was designed. It can complete the flower thinning operation within a specified range by being mounted on a robotic arm. Meanwhile, a prototype of the flower thinning end effector was fabricated, and field tests were conducted to verify its operational performance.

MATERIALS AND METHODS

Design of the End Effector

The end effector mainly consists of a motor, support base, flower-thinning shaft support, flower-thinning shaft, guide rail, bi-directional lead screw, flower-thinning spring piece, and comb-teeth column. The bi-directional lead screw is fixed to the base, the flower-thinning shaft support is fixed to the bi-directional lead screw, and the comb-teeth column is fixed to the flower-thinning shaft support. The flower-thinning shaft is connected to the drive motor via a coupling. Its 3D model is shown in Figure 1.

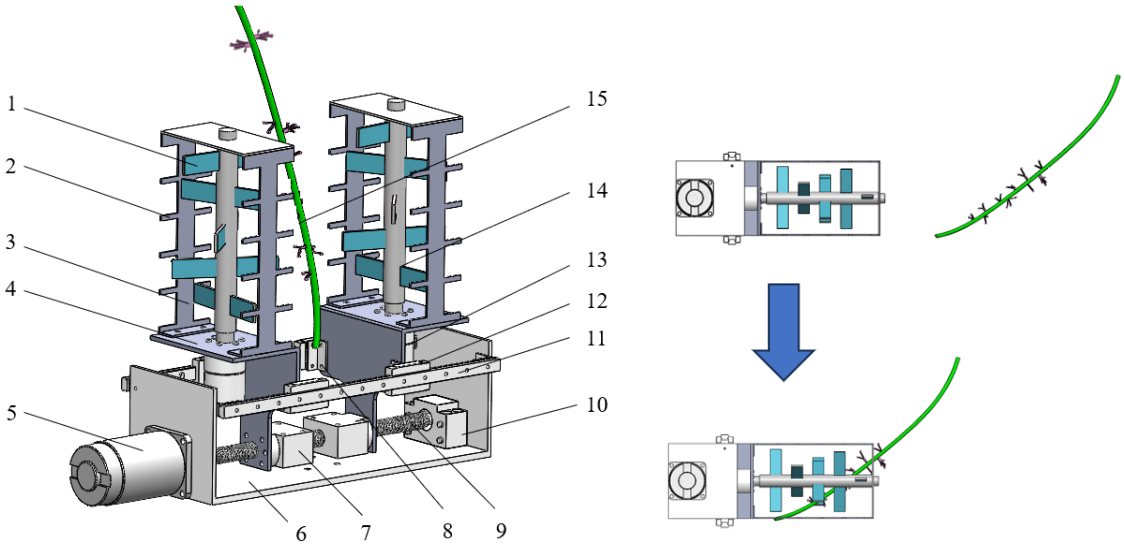

(a) End effector (b) End effector work process

Fig. 1 - 3D diagram of the end effector and its working principle

1) Flower thinning spring piece; 2 - Comb teeth; 3 - Comb teeth column; 4 - Flower thinning shaft base; 5 - Lead screw motor; 6 – Base; 7 - Lead screw nut; 8 - Angle iron; 9 - Bi-directional lead screw; 10 - Lead screw base; 11 - Guide rail; 12 - Guide rail support; 13 - Flower thinning shaft motor; 14 - Flower thinning shaft; 15 – Branch

The working principle is as follows: during the flower thinning operation, the flower clusters are identified by the visual recognition system. Under the control of the system, the robotic arm moves the end effector to the appropriate position, as shown in Figure 1. The motor drives the bi-directional lead screw to move the flower thinning shaft to the appropriate position, exerting a fixed effect on the branches. The flower thinning shaft motor is then activated, causing the flower thinning spring piece to rotate. Some flowers fall off due to the shear force when they come into contact with the spring pieces.

The remaining flowers, under the limiting effect of the comb teeth, are positioned at the front end in the direction of rotation. The flower pedicels are within the gap between the flower thinning spring piece and the comb teeth. As the flower thinning spring piece moves forward during rotation, the flower pedicels trapped between the comb teeth are better subjected to the shear force exerted by the spring piece. The flowers fall off due to the shear force. During this process, multiple spring pieces on the two flower thinning shafts perform flower thinning work simultaneously. After all flowers in the working area have been thinned, the system moves to the next thinning point, continuing until the entire flower thinning operation is complete. The process of flower removal by the spring piece is shown in Figure 2.

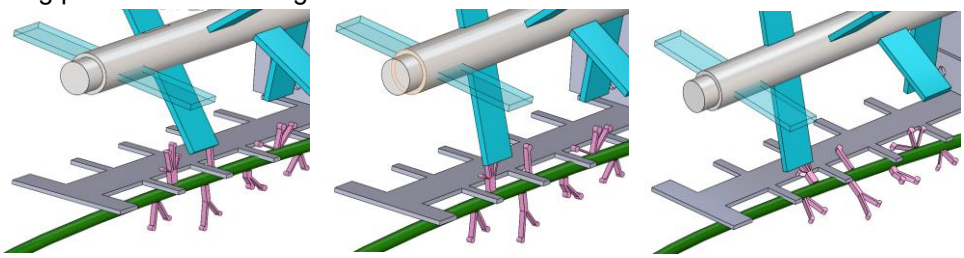

(a) (b) (c)

Fig. 2 - Schematic diagram of flower thinning

(a) Flower entering the comb teeth; (b) Spring piece contacts the flower; (c) The flower pedicel gradually breaks

Force Analysis of Key Components in the Flower Thinning Process

During the flower thinning operation, the flower thinning shaft drives the flower thinning spring piece to rotate, causing it to interact with the flowers, flower pedicels, and branches of the fruit tree. To facilitate the analysis of this process, the flower model is simplified into a force model used in engineering. According to engineering analysis theory, it can be considered that external shear forces cause the flower pedicel to break, allowing the flowers to fall off the branches. When the flower thinning spring piece makes contact with the flower pedicel, the instantaneous force applied to the flower pedicel can be approximated as a uniform force. Since the contact area of this force is much smaller than the surface area of the flower pedicel, it can be regarded as a concentrated force acting at a specific point on the flower pedicel. In the force model of the flower, the connection node between the flower pedicel and the branch is regarded as a fixed end. When the force is applied to the contact point on the flower pedicel, it will deform in the direction of the applied force. When the deformation exceeds a certain threshold, the structure of the flower pedicel will experience displacement, eventually leading to the breakage of the flower pedicel. During the entire flower thinning process, the flower thinning spring piece must not only bear its own weight but also overcome work resistance, centrifugal force, and the frictional resistance generated during the cutting of the flower pedicel by the spring piece. Considering that work resistance, centrifugal force, and other factors significantly affect the performance of the components during operation, a simplified model of the flower thinning device is used for force analysis. In this simplified model, point b is the center of mass of the spring piece, point d is the farthest end of the spring piece from the shaft, point c is the contact point between the spring piece and the flower pedicel, and point a is the fastening point between the flower thinning spring piece and the flower thinning shaft. Using the impulse-moment theorem and D'Alembert's principle, an in-depth analysis of the forces acting on the flower thinning component when it contacts the flower pedicel is conducted, and the following conclusions can be drawn.

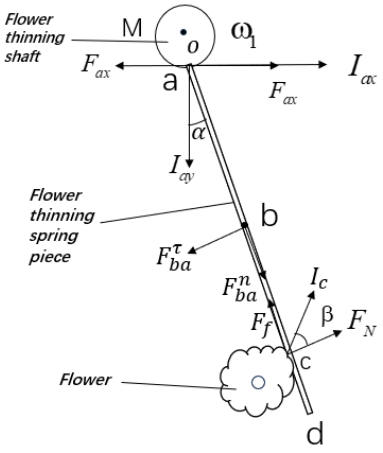

Fig. 3 - Schematic diagram of the force of the flower thinning component

$$\begin{cases} I_{ay}\sin\alpha - I_{\alpha x}\cos\alpha - I_{c}\cos\beta = m_2(\omega_2^{'} - \omega_2)L_x \\ J(\omega_2^{'} - \omega) = I_{\alpha y}\sin\alpha L_{\alpha b} - I_{\alpha x}\cos\alpha L_{\alpha c} - I_{c}L_{oc}\cos\beta \\ M - F_{\alpha x}L_{o\alpha} = 0 \\ F'_{\alpha x} + F^{\tau}_{b\alpha}\cos\alpha - F^{n}_{b\alpha}\sin\alpha + F_f\sin\alpha - F_N\cos(\alpha+\beta) = 0 \\ J_b a^{'}{}_2 + F^{\tau}_{b\alpha}L_{\alpha b} + F^{\tau}_{b\alpha}L_{\alpha b}\sin\alpha - F_N(L_{\alpha b} + L_{bc})\cos\beta + \frac{1}{2}F_y\delta = 0 \\ \omega_1 L_{o\alpha}\cos\alpha - \omega^{'}{}_2 L_{\alpha c} - V_m\cos\alpha = 0 \end{cases} \quad (1)$$

M is the torque of the flower thinning shaft, $N{\cdot}m$. ω_1 is the angular velocity of the flower thinning shaft, rad/s. m_2 is the mass of the spring piece, kg. β is the angle between the spring piece and the vertical direction of the plane, °. r is the angle between the direction of the collision impulse and the collision surface, °. ω_2 is the angular velocity of the spring piece before colliding with the flower pedicel, rad/s. ω_2' is the angular velocity of the spring piece after colliding with the flower pedicel, rad/s. I_{ax} is the horizontal component of the impulse exerted by the spring piece on point A, $N{\cdot}S$. I_{ay} is the vertical component of the impulse exerted by the spring piece on point A, $N{\cdot}S$. I_c is the impulse exerted by the spring piece on point C, $N{\cdot}S$. F_{ax} is the horizontal constraint force acting on point A, $N{\cdot}S$. F_N is the working resistance force of the spring piece, N. F_{ba}^{n} is the tangential adhesive force of the spring piece, N. F_{ba}^{τ} is the normal adhesive force of the spring piece, N. F_f is the frictional force generated between the spring piece and the flower pedicel leaf, N. L_{ad} is the length of the spring piece, m. L_{ab} is the distance from the hinge point of the spring piece to its center of mass, m. L_{oa} is the distance from the hinge point of the spring piece to the center of the thinning axis, m. L_{bc} is the distance from the contact point of the spring piece with the flower pedicel to its center of mass, m. a_2' is the acceleration of the spring piece after collision with the flower pedicel, m/s^2. J_c is the moment of inertia of the spring piece, $kg \cdot m^2$.

Due to the rotational operation of the spring piece on the flower thinning shaft during the process, in order to improve work efficiency, the impulse at the fastening point between the flower thinning spring piece and the flower thinning shaft is considered to be zero. Substituting this into the equation yields the following result.

$$L_{bc} = \frac{J_c}{m_2 L_{ab}} \quad (2)$$

$$F_N = \frac{(J_b + m_2L_{ab}^2)(m_2\omega_2 L_{ab}\sin\alpha - \frac{M}{L_{o\alpha}}) + m_2L_{ab}^2\sin\alpha\cos\alpha m_2\omega_1^2 L_{oa}}{m_2L_{\alpha b}\cos\alpha(L_{\alpha c} - \frac{1}{2}f\delta) + [J_b + m_2(L_{ad} + L_{bd})^2](\cos\alpha - f\cos\alpha)} \quad (3)$$

$$\omega^{'}{}_2 = \frac{\omega_1 L_{o\alpha}\cos\beta - V_m\cos\beta}{L_{\alpha b}} \quad (4)$$

Through force analysis of the flower thinning component, it can be determined that the impact position of the spring piece on the flower pedicel is related to the rotational inertia J_c, the mass of the spring piece m_2, and the position of the center of mass. The impact force of the spring piece on the flower pedicel is influenced by parameters such as the angular velocity of the flower thinning shaft ω_1, the mass of the spring piece m_2, the length of the spring piece L_{ad} and the torque M.

Different Work Processes of the Flower Thinning Operation and Flower Force Analysis

When the flower thinning shaft drives the spring piece to operate, the flower thinning spring piece strikes the flower, causing it to fall off. The force-induced flower detachment can be divided into two situations.

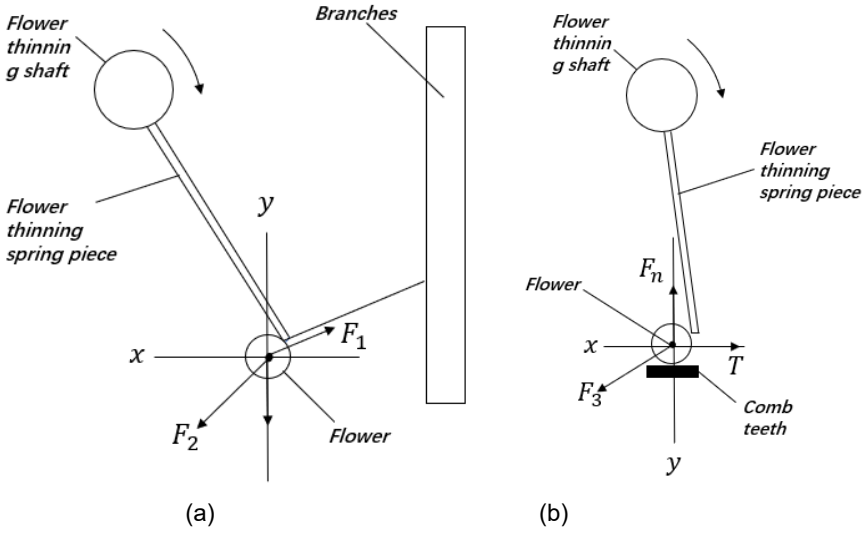

Fig. 4 - Force analysis of the flower under different working conditions

(a) Working condition 1. Simplified diagram of flower stress; (b) Working condition 2. Simplified diagram of flower stress

When a few flowers are only affected by the flower thinning spring piece and are knocked off, the flower pedicel comes into contact with the spring piece and is straightened. At this moment, the flower and the spring piece are relatively stationary, and the force is balanced. The flower is subjected to shear and frictional forces from the spring piece. The force diagram for this scenario is shown in figure 4.

When the flower thinning shaft rotates at a constant angular velocity ω, the speed at which the flower thinning spring piece strikes the flower is:

$$v_1 = \omega R \tag{5}$$

In the equation, R represents the distance from the flower to the flower thinning shaft, m.

At this moment, the acceleration at the force application point on the flower is:

$$a_1 = \frac{v_1^2}{R} = w^2 R \tag{6}$$

The impact force of the spring piece on the flower is:

$$F_2 = M_1 a_1 = M_1 w^2 R \tag{7}$$

In the equation, M_1 represents the mass of the spring piece, N.

When there is no relative displacement between the flower and the branch, the flower is in force equilibrium, and the force acting on the flower in the horizontal direction is:

$$F_2 \sin\theta_1 = F_1 \sin\theta_2 \tag{8}$$

In the equation, θ_1 is the angle between F_2 and the y-axis, θ_2 is the angle between F_1 and the y-axis, and F_1 is the force exerted by the flower pedicel on the flower, N.

When the flower thinning shaft drives the spring piece to rotate and the rotation speed exceeds a certain value, the connection point between the flower and the flower pedicel experiences a fracture under the action of shear force, causing the flower to fall off.

In actual flower thinning operations, due to the good elasticity of the flower pedicel, the force exerted by the spring piece often cannot completely detach the flower. Therefore, under the action of the comb teeth, a limiting effect is applied to the flower and pedicel, allowing the flower to better receive the force from the spring piece. The flower is subjected to the combined effect of the spring piece and the comb teeth. The force diagram is shown in figure 4.

When the flower thinning shaft rotates at a constant angular velocity ω, the speed at which the flower thinning spring piece strikes the flower is:

$$v_2 = \omega R_1 \tag{9}$$

In the equation, R_1 represents the distance from the flower to the flower thinning shaft, m

At this moment, the acceleration at the force application point on the flower is:

$$a_2 = \frac{v_2^2}{R_1} = w^2 R_1 \tag{10}$$

The impact force of the spring piece on the flower is:

$$F_3 = M_1 a_2 = M_1 w^2 R_1 \tag{11}$$

In the equation, θ_3 is the angle between F_3 and the y-axis.

The frictional force T exerted by the comb teeth on the flower is the resultant force in the horizontal direction.

$$T = \mu F_3 \sin\theta_3 = \mu M_1 w^2 R_1 \sin\theta_3 \tag{12}$$

In the equation, μ represents the coefficient of friction between the comb teeth and the flower, N.

When there is no displacement between the flower and the branch, the flower is in force equilibrium, and the force acting on the flower in the vertical direction is:

$$F_3 \cos\theta_3 + G = F_n \tag{13}$$

When the horizontal shear force applied to the flower exceeds a certain value, the flower falls off.

Through the force analysis of the flower thinning working components and the flower under different operating conditions, it can be concluded that when the material is fixed, the impact force exerted by the spring piece on the flower pedicel is related to parameters such as the angular velocity ω_1 of the flower thinning shaft, the mass M of the spring piece, the length L_{ad} of the spring piece, and the torque M. The greater the normal force F_N, the better the thinning performance of the spring piece on the flower, which is more favorable for the flower thinning operation.

Design of Relevant Parameters for the End Effector

When designing the overall dimensions, it is necessary to consider the actual situation of the flowers and fruit trees. Research was conducted in the orchard, and flower samples were taken. Measurements showed that the flower diameter ranges from 26 to 35 mm, and the flower pedicel length ranges from 28 to 56 mm. Based on this data, to ensure that the spring piece can effectively remove the flowers while leaving a certain parameter margin, the size of the flower thinning spring piece is designed to be 65 mm in length and 32 mm in width. The choice of material for the spring piece is also crucial.

For this study, the material used for the flower thinning spring piece is polypropylene, which ensures effective flower thinning while minimizing damage to the branches.

The flower thinning shaft plays a role in driving the spring piece in flower thinning operations. It is one of the key components and major force-bearing parts of the operation, and its structural design has a significant impact on the operational outcome. Its mass should be as small as possible, so a hollow tube is selected as the material for the flower thinning shaft. To improve flower thinning efficiency, the length is set at 260 mm, which is twice the distance between flower clusters. Five flower thinning spring pieces are evenly installed on the shaft, with a certain gap between each pair of spring pieces, ensuring that the flower removal rate reaches about fifty percent, as required by agricultural standards. When determining the arrangement of the spring pieces on the flower thinning shaft, a rotary tiller-like arrangement was used, so the spring pieces are arranged in a spiral pattern on the shaft, as shown in Figure 5.

During one full rotation of the flower thinning shaft, only one spring piece is at the same phase angle at a time. This ensures that the torque is more balanced, reduces torque fluctuations, increases operational stability, and ensures even load distribution. The flower thinning spring pieces have a certain width and a reasonable arrangement to minimize the occurrence of missed hits.

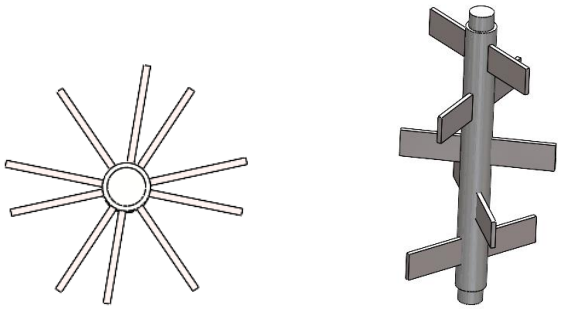

(a) (b)

Fig. 5 - Arrangement of spring plates on the thinning shaft

(a) Top view of the flower thinning mechanism; (b) Axonometric view of the arrangement

Simulation Analysis of Key Flower Thinning Components

It has been measured that the shear force range for the apple flower pedicel fracture is 3.69–4.79 N, with an average shear force of 4.18 N. To simulate the working process of the flower thinning end effector and analyze the impact force exerted by the spring piece on the flower at different rotational speeds, an ADAMS rigid-flexible coupling simulation analysis is performed on the end effector. During flower thinning operations, the flower thinning device must have a certain level of stiffness and flexibility to ensure effective flower thinning while minimizing damage to the branches. In this simulation, polypropylene is selected as the material for the spring piece, while the other components are made of aluminum. Then, constraints are applied to the model based on the motion relationships between the various parts of the flower thinning machine. Figure 6 shows the diagram of the applied constraints.

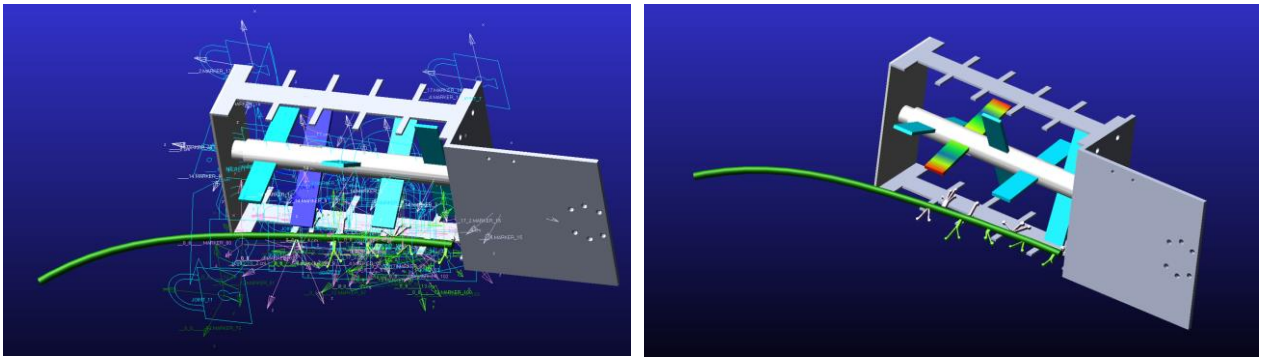

(a) (b)

Fig. 6 - ADAMS simulation

(a) Schematic diagram of constraint application; (b) Spring piece flexible settings

To simplify the flexible dynamics simulation model, based on the periodic repetitive impact characteristics of the flower thinning spring piece, one spring piece system on one side of the flower thinning shaft is selected as the research object. The model is constrained and driven based on the actual motion state of the flower thinning mechanism. The applied constraints are shown in Table 1.

Table 1

Constraint conditions

Serial number	Kinematic pair	Constrained components
1	Rotary pair	Flower thinning shaft + flower thinning shaft base
2	Fixed pair	Comb-tooth column + flower thinning shaft base
3	Fixed pair	Flower thinning spring piece + flower thinning shaft

RESULTS

Simulation results and data

The rotational speed of the flower thinning shaft was set to 150-250 r/min. Based on the relatively low geometric complexity of the mechanism, the ADAMS/Flex module was used to generate a flexible body: in the ViewFlex module, the spring piece that needed to be made flexible was selected, with the material defined as polypropylene. The flexible body type was set to geometric appearance, with entity mesh parameters having a reference size of 5 mm, a minimum element size of 1 mm, and a size gradient coefficient of 1.5. The remaining options were kept at their default values. After performing mesh division, flexible body creation was completed through automatic contact point recognition, and the final output was the flexible model of the polypropylene material flower thinning spring piece, showing its nonlinear deformation characteristics. The spring piece's flexibility was shown in Figure 6.

The flower thinning spring piece, after undergoing flexible treatment, made contact and collided with the branches and flowers. Due to the inertia and elasticity of the flower thinning spring piece, swinging occurred after it underwent flexible deformation. Subsequently, the flower thinning spring piece continued to rotate under the drive of the flower thinning shaft.

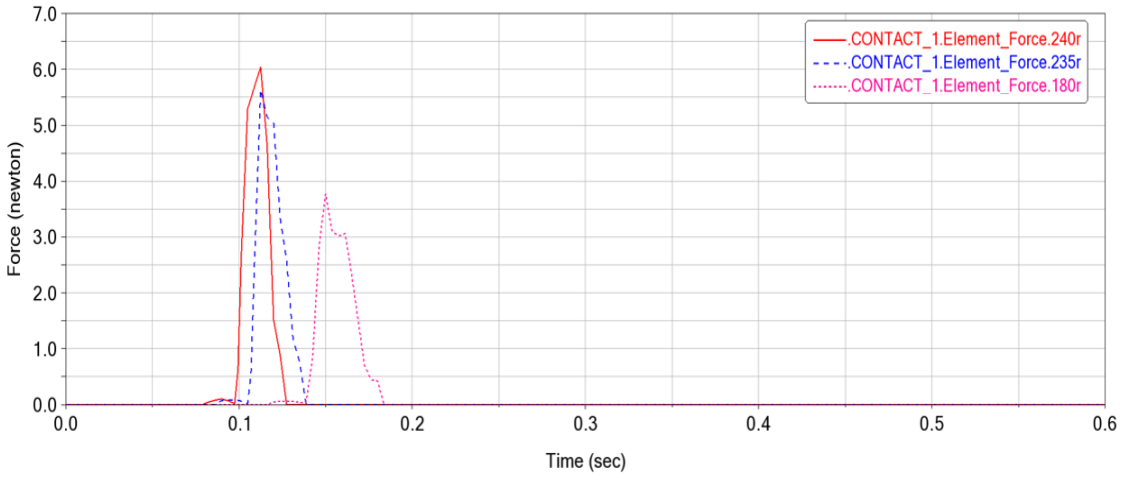

Fig. 7 - Contact force curves of spring piece at different speeds

Table 2

Impact force simulation results

Rotational speed / $r \cdot min^{-1}$	150	180	230	235	240	250
Applied force / N	2.76	3.82	4.91	5.59	5.98	6.76

The rotational speed range of the flower thinning shaft was set between 150 r/min and 250 r/min. The contact force of the flower thinning spring piece was calculated through simulation. The simulation results were shown in Table 2. From Table 2, it could be seen that the contact force increased as the rotational speed increased. From Figure 7, it was clear that when the rotational speed was at 180 r/min, during the stage when the flower thinning spring piece had not yet come into contact with the flower, the force remained at 0. At 0.14 s, the flower thinning spring piece began to contact the flower, and the contact force gradually increased, reaching a peak value of 3.82 N. However, the force still did not meet the flower thinning standards.

When the rotational speed of the flower thinning shaft reached 240 r/min, the flower thinning spring piece made contact with the flower at 0.09 s, and the contact force gradually increased to 5.98 N. The simulation results showed that at lower rotational speeds, the force curve fluctuated significantly within a short period and even produced several force peaks. However, at higher rotational speeds, the force curve was more stable with only one peak. Analysis indicated that at slower rotational speeds, the simulation process was slower, and after the flexible flower thinning spring piece contacted the target, certain deformation occurred, leading to multiple force peaks detected at the contact point. When the deformation exceeded the maximum value, the flower thinning spring piece completed the impact on the target and continued to rotate.

The maximum force value in the curve represented the accurate force under that rotational speed. Based on the previous analysis, the range of shear force required to break the apple flower's pedicel was between 3.69 N and 4.79 N. During the flower thinning operation, the force exerted by the flower thinning spring piece had to be greater than 4.79 N. When the rotational speed of the flower thinning shaft was between 230 and 250 r/min, it met the force requirements for the flower thinning operation.

Prototype Manufacturing and Field Testing

To evaluate the performance of the end effector, based on the analysis and parameter optimization results of the various components of the whole machine mentioned earlier, the flower thinning end effector was modeled using 3D design software. The rationality of each component was checked, and the prototype was manufactured for testing.

In this study, the manufactured prototype was installed at the end of the robotic arm. During operation, a binocular camera captured the overall information of the fruit trees, and the central control machine analyzed and processed the information. After processing, it provided the solution and working coordinates. The robotic arm, upon receiving the coordinates of the working position via internal communication, moved to the designated point. The motor of the end effector started rotating to remove the flowers that needed thinning. Afterward, it moved to the next position point that required flower thinning, repeating the operation. After completing the flower thinning for one fruit tree, the entire machine moved to the next fruit tree and repeated the process. The movement between trees was mapped in advance by radar, allowing for fixed-point cruising of each tree in the orchard. After completing the entire orchard or a row of trees, the machine moved to the set orchard origin point and waited.

Fig. 8 - Field experiment on flower thinning

Fig. 9 - End Effector in field operation

To verify the flower thinning effect of the end effector and assess the rationality of the end effector's structure, the flower thinning rate was calculated, and field tests were conducted on the end effector. After completing the operation, the flower thinning rate for each branch was calculated, which was the ratio of the remaining flowers on each branch before and after flower thinning.

The calculation formula is

$$k = 1 - \frac{Z_1}{Z} \times 100\% \tag{14}$$

where Z_1 is the number of remaining flowers after the operation is completed, and Z is the original number of flowers on the branch.

Table 3

Test results of flower thinning and branch damage rate

Branch number	Number of flowers/piece	Number of flowers thinned/piece	Thinning rate/%	Branch surface area/mm²	Damage area/mm²	Damage rate/%
1	22	13	59.1	783.91	27.43	3.5
2	16	7	43.8	652.37	9.89	1.5
3	23	10	43.4	897.04	11.66	1.3

Branch number	Number of flowers/piece	Number of flowers thinned/piece	Thinning rate/%	Branch surface area/mm²	Damage area/mm²	Damage rate/%
4	9	5	55.6	615.28	17.23	2.8
5	19	9	47.4	848.75	30.56	3.6
6	13	7	53.8	721.59	11.53	1.6
7	19	10	52.6	669.43	15.39	2.3

To ensure accuracy in the experiment, multiple branches from different plants were selected. During flower thinning, it was also important to ensure that the branches were not damaged by the end effector's operation. Based on previous experience and expert advice, the epidermal damage area of the branches was kept to less than 4% of the total area of the branch. The rotational speed of the flower thinning shaft was set to 240 r/min, and the following results were obtained through the experiment.

According to agronomic requirements and past experience, a flower thinning rate of around 50% was considered the optimal thinning rate. As shown in Table 3, this basically met the agronomic requirements for flower thinning.

CONCLUSIONS

This study presents the design of an orchard flower thinning machine equipped with a comb-tooth end effector, developed according to the physical properties of flowers and the requirements of the thinning process. The thinning method combines spring pieces with comb teeth. By optimizing the size of the spring pieces, selecting suitable materials, and analyzing their force characteristics during operation, as well as the mechanical response of flowers under different working conditions, the key factors influencing flower detachment were identified. Through ADAMS rigid-flexible coupled dynamic simulation, the optimal rotational speed range of the end effector's key components was determined to be 230-250 r/min. Field experiments confirmed that the design met agronomic requirements for flower thinning. Overall, the results demonstrate that the proposed design provides effective technical support for improving the efficiency and precision of flower-thinning operations in orchards.

ACKNOWLEDGEMENT

This research was funded by the National Natural Science Foundation of China (No:31971801), the Natural Science Foundation of Shandong Province of China (No: ZR2020ME252, ZR2020ME250) and Qingdao Science and Technology Benefit-the-People Demonstration Project(25-1-5-xdny-33-nsh).

REFERENCES

[1] Alberto A., Daniela G., Mattia C., Sandro S., Gianluca B., Giuseppina C. (2018). Evaluation of a new machine for flower and fruit thinning in stone fruits. *Sustainability*, Vol. 10, pp. 4088-4088, Italy.

[2] Chen G., Li J., Chen H., An Y. (2018). Research Progress of Artificial Intelligence Technology in the Agricultural Field in the Era of Big Data (大数据时代人工智能技术在农业领域的研究进展), *Journal of Jilin Agricultural University*, Vol. 40, pp. 502-510, Jilin/China.

[3] Cheng D., Chen J., Gu H., (2018). Efficient and Labor-Saving Grape Clusters Thinning Technology (葡萄省工高效整穗疏果技术), *Fruit Grower's Friend*, Vol. 04, pp. 13-14, Henan/China.

[4] Cheng D., He S., Li M., (2020). The Effect of Different Flower Cluster Shaping Methods on the Fruit Quality of Zhengyan Seedless' Grapes (不同花穗整形方式对'郑艳无核'葡萄果实品质的影响), *China Fruit Trees*, Vol. 04, pp. 18-22, Henan/China.

[5] Cheryl H., Karen B., (2011). Efficacy of blossom thinning treatments to reduce fruit set and increase fruit size of Ambrosia and Aurora Golden Gala apples. *Canadian Journal of Plant Science*, Vol. 91, No. 6, Canada.

[6] Dennis H., Ines H., Karen L., Jim M., Michael B. (2011). Mechanical flower thinning improves fruit quality of apples and promotes consistent bearing. *Scientia Horticulturae*, Vol. 134, pp. 241-244, United States.

[7] Kang M., Wang X., Hua J., Wang H., Wang F. (2019) Parallel Agriculture: Intelligent Technologies Leading to Smart Agriculture (平行农业:迈向智慧农业的智能技术), *Journal of Intelligent Science and Technology*, Vol. 1, pp. 107-117, Shandong/China.

[8] Lan Y., Wang T., Chen S., D. (2020). Agricultural Artificial Intelligence Technology: The Wings of Modern Agricultural Science and Technology (农业人工智能技术: 现代农业科技的翅膀), *Journal of South China Agricultural University*, Vol. 41, pp. 1-13, Guangdong/China.

[9] Lei X., Yuan Q., Xyu T., Qi Y., Zeng J., Huang K., Sun Y., Herbst A., Lyu X. (2023). Technologies and Equipment of Mechanized Blossom Thinning in Orchards: A Review. *Agronomy*, Vol. 13, Jiangsu/China.

[10] Li J., Xu Y., Xu J., Yang Z., Lu H. (2016). Design and Experiment of Control System for Suspended Electric Flexible Flower Thinning Machine (悬挂式电动柔性疏花机控制系统设计与试验), *Transactions of the Chinese Society of Agricultural Engineering*, Vol. 32, pp. 61-66, Guangdong/China.

[11] Liu H., Chi J., Liang Q., Liu T., Wang H., Li S., Hu C. (2025). Design and Simulation Analysis of a Crawler-type Double-arm Apple Flower Thinning Machine (履带式双节臂苹果疏花机的设计与仿真分析), *Journal of Agricultural Mechanization Research*, Vol. 47, pp. 35-41, Shandong/China.

[12] Liu L., Nie L., Zhao H., Cao Y., Sun A., (2018). Research on the Technical Issues of Apple Flower Thinning and Fruit Thinning (苹果疏花疏果技术问题研究), *Shaanxi Agricultural Science*. Vol. 64, pp. 88-91, Shaanxi/China.

[13] Lyons D. J., Heinemann P. H.; Schupp J. R., Baugher T. A., Liu J. (2015). Development of a selective automated blossom thinning system for peaches. *Transactions of the ASABE*, Vol. 58, pp. 41-42, United States.

[14] Matache M. G., Cristea R., Zaica A., Ciupercă R., Iosif A., Voicu Gh. (2024). Real-time mechanical flower thinning equipment, controlled by artificial intelligence, *INMATEH Agricultural Engineering*, Vol. 74, No. 3, pp. 875-884.

[15] Pan Y., Zhou Y., He L., Wang Q., Song Z., Song L., (2021). Research Progress on Flower Thinning and Fruit Thinning in Orchard Management (果园管理工作中疏花疏果的研究进展), *Journal of Agricultural Mechanization Chemistry*, Vol. 42, pp.198-204, Xinjiang/China.

[16] Robinson T.L., Lakso A.N., (2011). Predicting chemical thinner response with a carbohydrate model. *Acta Horticulturae*, Vol. 903, pp.743-750.

[17] Sui S., Li M., Li Z., Zhao Y., Wang C., Du W., Li X., Liu P. (2024). A comb-type end-effector for inflorescence thinning of table grapes. *Computers and Electronics in Agriculture*, Vol. 217, Shandong/China.

[18] Wang L., Liu R., (2020). The Effect of Different Cluster Thinning Methods on the Quality of Facility-Grown Red Baraldo Grapes (不同整穗方式对设施葡萄红巴拉多品质的影响), *Agriculture and Technology*, Vol. 40, pp. 41-43, Gansu/China.

[19] Wang Q. (2018) *Design and Research of Flower Thinning Device for Dwarf Dense Fruit Trees* (矮密果树疏花装置设计及研究), Hebei Agricultural University, Master's Thesis, Hebei/China.